Principles for circadian orchestration of metabolic pathways

Kevin Thurley[a,b,c], Christopher Herbst[b,1], Felix Wesener[a,1], Barbara Koller[b], Thomas Wallach[b], Bert Maier[b], Achim Kramer[b], and Pål O Westermark[a,2,3]

[a]Institute for Theoretical Biology, Charité–Universitätsmedizin Berlin, 10115 Berlin, Germany; [b]Laboratory of Chronobiology, Institute for Medical Immunology, Charité–Universitätsmedizin Berlin, 10117 Berlin, Germany; and [c]Department of Pharmaceutical Chemistry, University of California, San Francisco, CA 94158-2330

Edited by Joseph S. Takahashi, Howard Hughes Medical Institute, University of Texas Southwestern Medical Center, Dallas, TX, and approved December 23, 2016 (received for review August 10, 2016)

Circadian rhythms govern multiple aspects of animal metabolism. Transcriptome-, proteome- and metabolome-wide measurements have revealed widespread circadian rhythms in metabolism governed by a cellular genetic oscillator, the circadian core clock. However, it remains unclear if and under which conditions transcriptional rhythms cause rhythms in particular metabolites and metabolic fluxes. Here, we analyzed the circadian orchestration of metabolic pathways by direct measurement of enzyme activities, analysis of transcriptome data, and developing a theoretical method called circadian response analysis. Contrary to a common assumption, we found that pronounced rhythms in metabolic pathways are often favored by separation rather than alignment in the times of peak activity of key enzymes. This property holds true for a set of metabolic pathway motifs (e.g., linear chains and branching points) and also under the conditions of fast kinetics typical for metabolic reactions. By circadian response analysis of pathway motifs, we determined exact timing separation constraints on rhythmic enzyme activities that allow for substantial rhythms in pathway flux and metabolite concentrations. Direct measurements of circadian enzyme activities in mouse skeletal muscle confirmed that such timing separation occurs in vivo.

circadian rhythms | glucose metabolism | metabolic response analysis | mouse skeletal muscle

Circadian rhythms are ∼24-h cycles in behavior, physiology, and cellular processes that persist in the absence of external cues. In mammals, circadian rhythms in the expression of thousands of genes in various metabolic tissues ensure up- or down-regulation of important metabolic processes in anticipation of daily activity and rest periods (1, 2). Circadian gene expression in mammalian tissues depends on the circadian core clock, a genetic feedback oscillator inducing the transcription of thousands of clock-controlled genes. Additional rhythmicity in gene expression is generated by rhythmic posttranscriptional regulation (3). Circadian rhythms have been detected in mRNA and protein abundances (4–6), enzyme activities (7, 8), and concentrations of metabolites (9–11) in various mammalian tissues. Whereas the mechanisms underlying rhythmic gene expression are relatively well-studied, it remains unclear how circadian gene expression induces rhythms in the abundance of metabolites or metabolic fluxes.

A naïve picture of circadian regulation (Fig. 1*A*) ("central dogma of molecular chronobiology") suggests that the circadian core clock drives rhythmic mRNA expression, resulting in rhythmic protein levels and directly leading to rhythmic enzyme activity (12) and thus, metabolic activity. Here, especially metabolic pathway flux (rate of conversion of substrate into product metabolites measured in concentration per time; an analogy is water flow through a floodgate) has been regarded as a crucial biological function under strong evolutionary selection pressure (13, 14). However, it is unclear whether circadian abundances of enzyme transcripts are widespread generators of circadian enzyme activities: Metabolic enzymes in general have long half-lives (15), which preclude circadian rhythms in abundance (3). Furthermore, it remains unknown how circadian rhythms in enzyme activities propagate to rhythmicity in metabolite concentrations and metabolic fluxes through entire pathways.

Here, we show that similar peak times of circadian enzyme activities in a metabolic pathway do not necessarily lead to high amplitudes in pathway fluxes. Rather, in many cases, separation in times of peak activity by several hours is advantageous for pronounced circadian rhythms, even when the individual metabolic reactions operate with fast kinetics. We developed a theoretical method called circadian response analysis (CRA) and derived exact rules for the circadian orchestration of important metabolic pathway motifs. We applied these insights to clarify circadian control of glucose metabolism in mouse skeletal muscle by analysis of gene expression data and direct measurement of circadian activities of glycolytic key enzymes.

Results

Circadian Rhythms in the Regulation of Enzymatic Activities. How do circadian rhythms propagate from transcripts to enzyme activities (Fig. 1*A*)? Mechanistically, rhythms could propagate either directly via rhythms in enzyme concentrations or through regulatory proteins that modulate enzyme activities in a circadian

Significance

Circadian (24-h) rhythms influence the behavior and physiology of many organisms. These rhythms are generated at the gene expression level, causing the waxing and waning of protein abundances. Metabolic enzymes are affected, but the principles for the propagation of enzyme rhythmicity to cellular metabolism as quantified by fluxes through metabolic pathways and metabolite concentrations are not understood. We used the mathematics of chemical kinetics to systematically investigate how rhythms in enzyme activity are propagated to pathway fluxes and concentrations. It turned out that rhythms are often optimally propagated when several enzyme activities are rhythmic but with different timing. We performed measurements of circadian enzyme activities in mouse muscle that confirmed such timing differences.

Author contributions: K.T., A.K., and P.O.W. designed research; K.T., C.H., F.W., B.K., and P.O.W. performed research; K.T., T.W., B.M., A.K., and P.O.W. contributed new reagents/analytic tools; K.T. and P.O.W. analyzed data; and K.T. and P.O.W. wrote the paper.

The authors declare no conflict of interest.

This article is a PNAS Direct Submission.

[1]C.H. and F.W. contributed equally to this work.

[2]To whom correspondence should be addressed. Email: westermark@fbn-dummerstorf.de.

[3]Present address: Institute of Genetics and Biometry, Leibniz Institute for Farm Animal Biology, 18196 Dummerstorf, Germany.

This article contains supporting information online at www.pnas.org/lookup/suppl/doi:10.1073/pnas.1613103114/-/DCSupplemental.

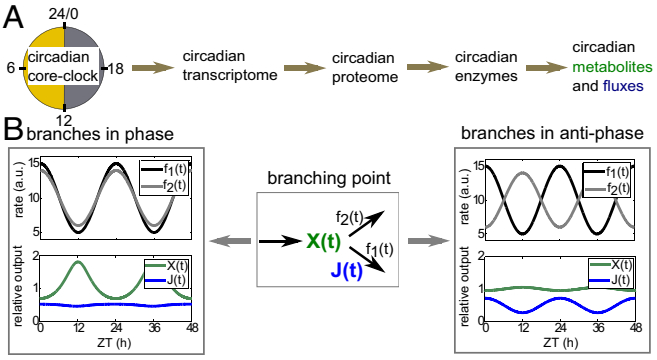

Fig. 1. Regulation of metabolic functions by the circadian clock. (*A*) Illustration of the central dogma of molecular chronobiology. The core clock generates rhythmic transcripts, which result in rhythmic proteins, enzyme activities, and metabolites and fluxes. (*B*) Simulation illustrating the effect of a circadian branch point. The two branching reactions with periodic rate coefficients $f_1(t)$, $f_2(t)$ (relative amplitudes 0.5 and 0.4, respectively) are either in phase or antiphasic as indicated. As a result, the metabolite $X(t)$ and flux $J(t)$ are either strongly rhythmic or constant. ZT, zeitgeber time.

fashion (16). Several studies have emphasized the direct mechanism by mapping rhythms in mRNA expression to metabolic enzymes and sometimes directly measuring enzyme activities (17–19). In a few cases, rhythmic mRNA and protein levels have been measured together with rhythmic enzyme activities (20), supporting this mode of rhythm propagation more rigorously. However, we noted that metabolic enzymes are generally long-lived proteins (15), and enzyme regulatory proteins have significantly shorter half-lives (Fig. S1*A*). Therefore, there are reasons to doubt that circadian rhythmicity in enzyme concentration is a widespread strategy to induce rhythmic enzyme activity, because long protein half-lives preclude circadian rhythms in protein abundance (3). Thus, regulatory proteins are more plausible mediators of rhythms, which should be considered when performing transcriptome- or proteome-wide studies.

In general, if enzyme activities are rhythmic, one may expect that the metabolites and fluxes of metabolic pathways become rhythmic, because metabolic rate coefficients are typically much faster than the circadian frequency $\omega = 2\pi/(24\text{ h}) \approx 0.26\text{ h}^{-1}$ (Fig. S1*B*). If several enzymes in a metabolic pathway have rhythmic activities, how do these translate to rhythms in metabolites and fluxes? As an illustration, we considered a branching point in a metabolic network (Fig. 1*B*). A metabolite X is produced with constant rate and processed by two independent reactions with rhythmically changing rate coefficients $f_1(t), f_2(t)$. The rhythms in the rate coefficients represent rhythms in enzyme activity. Such branching points are common in metabolism; an example is glycogen synthesis breaking off from the glycolytic pathway. Simulation with equal rate coefficients for all reactions showed that, if the two branching reactions are in phase, the metabolite concentrations are rhythmic with maximal relative amplitude (amplitude divided by mean; hereafter simply amplitude), but the fluxes through both branches are almost constant (Fig. 1*B*). Similarly, when the two reactions have opposite phases, the metabolite concentrations are constant [as long as average $f_1(t), f_2(t)$ do not differ too much as analyzed in-depth below], whereas the fluxes have maximal amplitude. Hence, the outcome of rhythmic enzyme activities at branching points strongly depends on their phases.

Metabolic Network Motifs Studied by CRA. The example of the branching point (Fig. 1*B*) shows that rhythmic enzymes do not necessarily result in both rhythmic metabolites and fluxes, and if they do, the metabolites and fluxes can widely differ in phase. This observation raises a number of questions. Can we predict the amplitudes and phases of metabolites and fluxes based on the properties of rhythmic enzymes? What are optimal phases of enzyme activity for synergistic induction of rhythms in metabolite concentrations and fluxes? Can we expect highly rhythmic metabolic fluxes given the complex regulation of metabolic networks? To address such questions quantitatively, we developed CRA, a theory based on an extension (21) of metabolic control analysis (MCA) (22–24) (*Materials and Methods* and Fig. S1*C*). Application of CRA resulted in simple formulas that describe amplitudes and phases of concentrations and fluxes caused by circadian enzyme activities (formulas listed in *SI Appendix* and Datasets S1 and S2).

Most metabolic networks can be decomposed into common motifs, such as linear chains, branching points, and cycles (25). Therefore, we used CRA to study the principles of rhythm propagation in such common network motifs (Fig. 2*A* and Fig. S2*A*). In each motif, we assumed that two enzyme activities are circadian with phases φ_1, φ_2, simplifying our analysis to the study of phase differences $\Delta\varphi = \varphi_2 - \varphi_1$. We computed the relative amplitudes of metabolites and fluxes in dependence of $\Delta\varphi$ (Fig. 2*B* and Fig. S2*B*), giving rise to the optimal phase difference $\Delta\varphi_{\text{opt}}$ in the sense of maximizing rhythms in the fluxes or concentrations, as well as the effect size S_{effect}, quantifying the importance of the phase difference (Fig. 2 *C* and *D* and Fig. S2 *C* and *D*). Our analytical results are close to simulations with linear kinetics (Fig. 2 and Fig. S2) as well as Michealis–Menten kinetics (Fig. S3 and Datasets S3–S5) in the physiological parameter regime (Fig. S1*B*).

The linear reaction chain is a classic network motif in metabolic pathway analysis and has been used to quantify control of glycolysis (22, 23, 26). Remarkably, we found that for linear chains, $\Delta\varphi_{\text{opt}}$ equals exactly 12 h for the metabolite $X(t)$ and 6 h for the outward flux $J(t)$, independent of kinetic parameters (Fig. 2*C*, "linear chain" and *SI Text*). Thus, rhythmic modulations of inward and outward reactions induce rhythmic fluxes with high amplitude not when the first and last reactions are in phase, but when the last reaction lags behind by around 12 (metabolite) or 6 h (flux)—we will refer to this result as the 12-/6-h rule of circadian metabolic reaction chains. Intuitively, the 12-/6-h rule can be understood by a floodgate analogy (Fig. S2*E*), where the water level (metabolite) is high when the gate (outward reaction) is closed, and the flow of water out of the basin (flux) is not maximal when the gate is at maximal size but when the water level is also high. For irreversible reactions, the effect size of the metabolite is close to its theoretical maximum of 1 for reasonable values of the average rate coefficient ($k_1 > 1\text{ h}^{-1}$), but the effect size of the flux vanishes, except for very small values of k_1 (Fig. 2*D*). In the floodgate analogy, this phenomenon stems from the water level going down at the same time as the floodgates open, so that both effects almost cancel out for the flux. Thus, in irreversible reactions, the 6-h rule has little effect on the flux, which for not too slow reactions is entirely determined by the input reaction.

Importantly, the effect of the 6-h rule on the flux increases if a reversible reaction (Fig. 2*D*) ("linear chain") or a storage metabolite (Fig. S2*D*) ("storage") is added. In the linear chain motif, higher effects of the output reaction on the flux are obtained for small equilibrium constants K_{eq} (i.e., in cases where "backward reactions" are faster) (Fig. 2*C*). Similarly, in the storage motif (e.g., lactate storage in glucose metabolism), an equilibrium shifted to the metabolite outside the chain leads to a higher effect size (Fig. S2*D*). In both cases (storage and chain), the additional equilibrium is analogous to an energy barrier, which the reaction chain has to overcome. In the floodgate analogy, this phenomenon corresponds to a more viscous fluid (e.g., honey or lava) instead of water (Fig. S2*F*), which induces a delay in the last reaction of the chain with respect to gate opening.

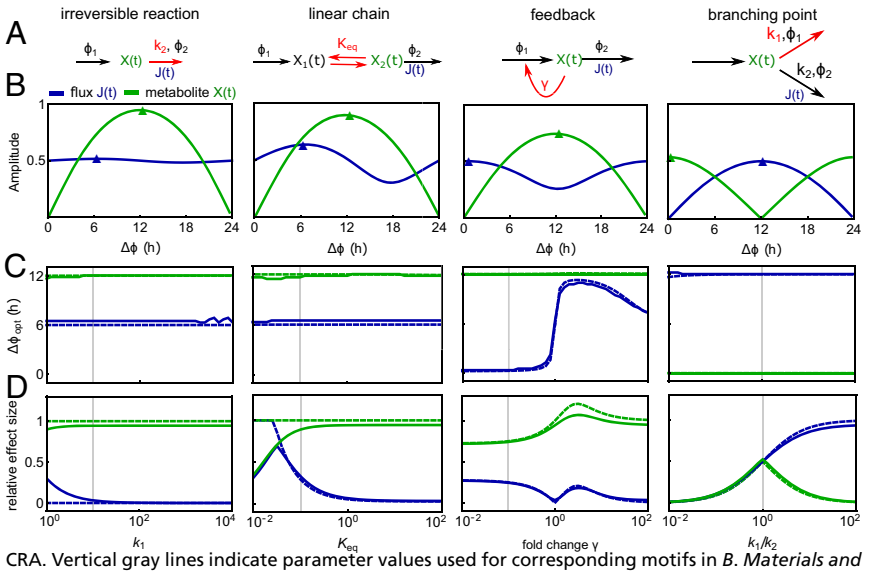

Fig. 2. Metabolic network motifs studied by CRA. (*A*) Model schemes. The reactions labeled φ_1, φ_2 are circadian with phase difference $\Delta\varphi = \varphi_2 - \varphi_1$; other reaction rate coefficients are constant. Red arrows and labels indicate the reaction and parameter value varied in the analysis. K_{eq} is the equilibrium constant; k_I is the inhibition constant. All models are described by mass action kinetics (*SI Appendix*). (*B*) Relative amplitudes of fluxes and metabolites depending on the phase difference $\Delta\varphi$. The value of the parameter determining the network motif (labeled in red in *A*) is indicated by gray vertical lines in *C* and *D* (see below). Small arrowheads indicate the peak phase derived analytically by CRA. (*C* and *D*) Optimal phase difference for high metabolite or flux amplitude $\Delta\varphi_{opt}$ (*C*) and effect size S_{effect} (*D*) for changing value of the parameter describing each network motif (*A*); in the linear chain motif ($K_{eq} = k_1^+/k_1^-$), k_1^+ was varied with $k_1^- = 300\ h^{-1}$, and in the branching point motif, k_2 was varied. Solid lines indicate numerical solutions, and dashed lines indicate analytical approximation based on CRA. Vertical gray lines indicate parameter values used for corresponding motifs in *B*. *Materials and Methods* shows standard parameter values.

In metabolic networks, linear chains are often accompanied by feedback regulation and branching points. We found that both positive and negative feedback increase the flux effect size for moderate feedback strength, at the same time modulating $\Delta\varphi_{opt}$ (Fig. 2 *C* and *D*, "feedback"). Interestingly, feedback does not change $\Delta\varphi_{opt}$ for the metabolites, and only positive feedback increases the metabolite effect size. For the branching point, as expected from the simulation in Fig. 1*B*, we found (Dataset S2 and *SI Appendix*) that $\Delta\varphi_{opt}$ equals 0 h for the flux through the branch in which the reaction is rhythmic and 12 h for the flux through the alternative branch (Fig. 2 *B* and *C*). Interestingly, the effect size is small for the metabolite if the average reaction coefficients of both branches differ substantially. There is, however, always a consistent effect of oscillations in both enzyme activities on the flux through at least one branch, even for large differences ($k_1 \gg k_2$). Notably, synergy does not take place in the branching point motif: amplitudes in the fluxes or the metabolite concentration never exceed the amplitudes of any of the individual enzyme activity rhythms (Fig. 2 *B* and *D* and *SI Text*).

The somewhat counterintuitive properties of branching points has important consequences for rhythmic control of metabolic cycles. On the 24-h timescale, cycles, such as the TCA (Fig. 3*A*) or urea cycles, generally have significant replenishment and removal fluxes [so-called anaplerotic and cataplerotic fluxes, respectively (27)]. Thus, a cycle can be described as a series of branching points (Fig. 3*B*). Considering a cycle with only one cataplerotic reaction and applying the quantitative description of branching points, we concluded that rhythmic activity of an enzyme in a cycle can only lead to one of two scenarios. (*i*) If there is cataplerosis from the rhythmically consumed metabolite, all fluxes and all metabolites, except the rhythmically consumed one, are rhythmic (Fig. 3*C*). (*ii*) If there is cataplerosis from one of the other metabolites, only the rhythmically consumed metabolite is rhythmic, and all other metabolites and all fluxes are nonrhythmic (Fig. 3*D*). In cases with several cataplerotic reactions, intermediate scenarios with strongly varying outcomes of enzyme activity may arise and can be expected (e.g., in the mouse liver TCA cycle, where several mitochondrial enzymes have rhythmic abundances) (28).

In summary, common network motifs often induce considerable delays between enzyme activities and the resulting metabolites and fluxes. Such delays may occur despite the fact that enzyme-catalyzed reactions operate at much faster timescales than the 24-h circadian rhythm, and even for arbitrarily fast reactions (Fig. 2*C* and Fig. S2*C*). As a consequence, phase differences between several rhythmic enzymes in a reaction cascade can increase the flux and metabolite amplitudes.

Gene Expression Patterns in Muscle Glucose Metabolism Reveal Circadian Regulation of Key Enzymes. After establishing the principles for circadian orchestration of metabolic network motifs, we asked to what extent such insights can be used in the study of physiologically important metabolic pathways. In particular, CRA revealed that phase lags between regulatory enzymes may be beneficial to obtain circadian fluxes and metabolites with appreciable amplitudes. Thus, we sought to investigate whether this is the case in a well-studied metabolic pathway, such as mammalian glucose metabolism. Notably, glucose metabolism operates quite differently in different organs. In mammalian

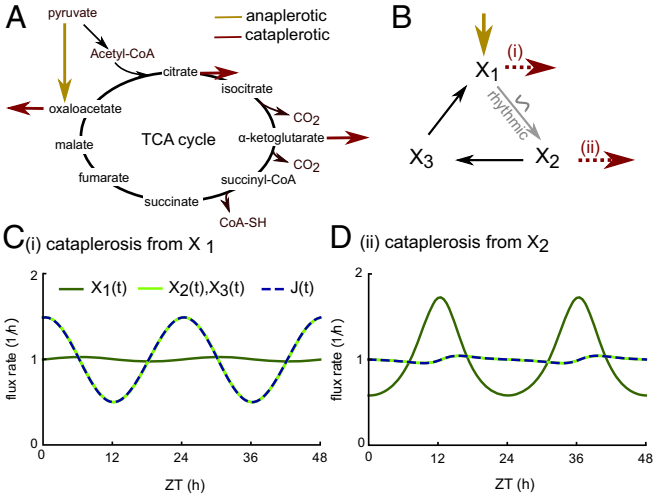

Fig. 3. Analysis of a circadian metabolic cycle. (*A*) Illustration of anaplerotic (material replenishment) and cataplerotic (material removal) reactions in the TCA cycle. (*B*) Model scheme of a cycle with an anaplerotic reaction and a cataplerotic reaction either before or after a rhythmically modulated reaction (details are in *SI Materials and Methods*). (*C* and *D*) Model simulations normalized to unit mean with a cataplerotic reaction at either the rhythmically consumed metabolite X_1 (*C*) or another metabolite (*D*; here X_2).

circadian biology, many of the available datasets on circadian gene expression focus on mouse liver. However, in this organ, the situation is complex [e.g., glycolysis and gluconeogenesis can both occur (29)]. To enable a more rigorous analysis, we instead focused on mouse skeletal muscle, where glucose, to a large extent, is either directly metabolized via glycolysis and subsequent TCA cycle reactions or stored as glycogen for times of high demand (29, 30) (Fig. 4*A*). Alternative routes, like the pentose phosphate pathway, account only for ∼2% of muscle glucose metabolism, whereas lactate accumulation and glycogenesis from lactate occur only during and after heavy exercise (30, 31), and gluconeogenesis is limited by the inability of muscle cells to export glucose.

Because circadian rhythms are primarily generated via rhythmic transcriptional activities, we investigated the circadian transcriptome of mouse skeletal muscle as reported in three independent studies (6, 18, 32). Applying standard criteria, we found that 15–20% of transcripts coding for enzyme regulatory proteins exhibited circadian rhythms as opposed to around 5% of transcripts coding for metabolic enzymes (in all datasets, $P \leq 0.05$, Fisher's exact test) (Fig. 4*B*). Moreover, by analyzing publically available protein half-life data (15), we found that enzyme regulatory proteins have significantly shorter half-lives (Fig. 4*C* and Fig. S4*A*) (Mann–Whitney rank sum test, $P < 0.008$) in a range permissive of circadian rhythms in protein concentration [i.e., below 50 h (3)]. Strikingly, in all three datasets (6, 18, 32), the transcripts *Pdk4* (pyruvate dehydrogenase kinase 4), *Pfkfb3* (6-phosphofructo-2-kinase/fructose-2,6-biphosphatase 3), and *Ppp1r3c* (protein phosphatase 1 regulatory subunit 3C) were circadian and interestingly exhibited markedly different phases. They were (except for *Pdk4* in ref. 6) in the top five of circadian transcripts associated with core metabolism with respect to relative amplitude (Fig. 4*D* and Fig. S4 *B* and *C*). They were also almost the only transcripts associated with metabolism showing a high amplitude (> 0.2) in all datasets (the only other transcript is *Ddit4,* which is part of a stress response pathway). The proteins coded by these three genes have a direct regulatory effect on key enzymes in glucose metabolism (Fig. 4*A*): PTG (the protein product of *Ppp1r3c*) stimulates glycogen synthesis, PFK2 (product of *Pfkfb3*) activates phosphofructokinase (PFK; the driving reaction of core glycolysis), and PDK4 inhibits the activity of pyruvate dehydrogenase (PDH; the irreversible reaction linking glycolysis and the TCA cycle) by phosphorylation. Hence, this analysis revealed a high likelihood that muscle glucose metabolism is subject to circadian oscillations.

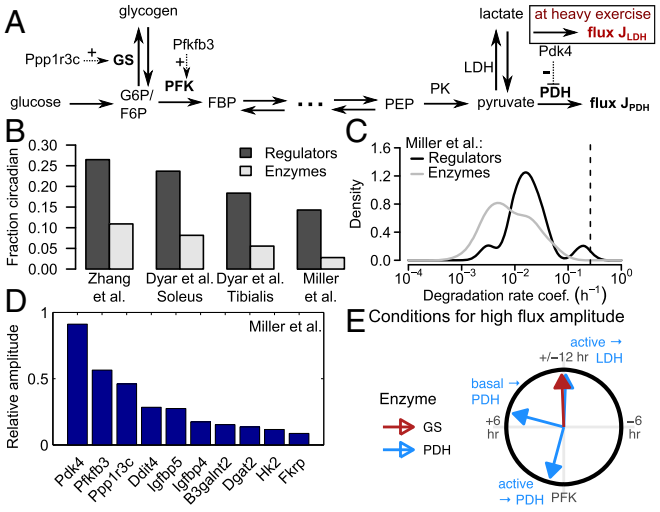

Fig. 4. Circadian activity in enzymes of muscle glucose metabolism. (*A*) Schematic network of mammalian muscle glucose metabolism. FBP, fructose-1,6-bisphosphate; F6P, fructose-6-phosphate; PEP, phosphoenolpyruvate; PK, pyruvate kinase. (*B–D*) Analysis of the three datasets [Miller et al. (32), Zhang et al. (6), and Dyar et al. (18) (separate data for soleus and tibialis)] of circadian gene expression in muscle metabolism. (*B*) Fraction of circadian genes. (*C*) Degradation rate coefficients (15) of expressed genes. (*D*) Circadian genes of carbon metabolism with highest relative amplitudes (in *C* and *D*) [Fig. S4 shows data from Zhang et al. (6), and Dyar et al. (18)]. (*E*) Constraints in $\Delta\varphi_{opt}$ between PFK (reference phase) and GS, or PFK and PDH, for a highly rhythmic glycolytic target flux through either PDH or LDH (see *SI Text* for details). The values result from a simple model (Fig. S5*A*) based on $\Delta\varphi_{opt} = 12$ h for the branching point in upper glycolysis (Fig. 2*D*) and an interval K_{eq} between 0.1 and 1 around our estimate for the overall equilibrium constant (Fig. S5*A* and Dataset S6).

In metabolic pathways, it is widely believed that the flux through a pathway is subject to evolutionary optimization, because it determines how fast energy and essential metabolites become available to the host organism (13, 33). This hypothesis certainly applies to the muscle, where fast energy availability is essential for adequate reactions to the environment. Indeed, at heavy exercise, the glycolytic flux is increased by orders of magnitudes within seconds (34). Therefore, we hypothesized that the circadian transcripts regulating enzyme activities in glucose metabolism might serve to generate rhythms in the glycolytic flux.

Muscle glucose metabolism can be described as a composition of three metabolic motifs (Figs. 2*A* and 4*A*) around three enzymes with activities that are most likely circadian: a branching point at glucose-6-phosphate [G6P; influx from glucose and glycogen and outflux through either PFK or glycogen synthase (GS)], a linear chain between G6P and pyruvate, and a storage metabolite or branching point right before the outflux through PDH and possibly, lactate dehydrogenase (LDH). The nature of the last motif depends on the model of glucose metabolism: At rest ("basal state"), lactate is not exported (34), and the glycolytic flux operates almost entirely through PDH, which yields the storage motif. At heavy exercise ("active state"), lactate is exported by the muscle and processed inside the liver (Cori cycle) (29, 34), resulting in the branching point motif. Based on these considerations, we developed a simplified mathematical model of glucose metabolism (Fig. S5 and *SI Text*) and derived conditions for high amplitudes of the glycolytic flux (Fig. 4*E*): PFK and GS should be in antiphase because of the branching point motif (Fig. 2*C*), and PDH should lag behind PFK by 1, 7, or 12 h depending on basal or active state and whether the flux through PDH or LDH is considered.

Circadian Enzymes Regulating Muscle Glucose Metabolism Have Widely Different Times of Peak Activity. Because enzymatic activities are delayed with respect to protein expression (3) and may depend on a variety of activating and deactivating factors, the gene expression profiles analyzed above can only serve as a first hint toward circadian activity of an enzyme, which must be determined directly by enzyme activity assays. We therefore turned to assess the circadian activity of the enzymes most likely contributing to a circadian glycolytic flux (GS, PFK, and PD) (Fig. 4*D* and Fig. S4*B*).

For this purpose, we assayed the change of activities of these enzymes over a 24-h period in mice entrained to a 24-h light/dark cycle (Fig. 5*A* and Fig. S6 *A* and *B*). To evaluate rhythmicity, we used two independent statistical methods: a nonparametric method implemented in the software package RAIN (35) and harmonic regression (3). *P* values were combined using Fisher's method (36). We found that PFK ($P = 0.0020$), PDH ($P = 7.8 \times 10^{9}$), and phosphoglycogen synthase (p-GS) ($P = 3.1 \times 10^{7}$), but not the housekeeping protein α-tubulin ($P = 0.50$), show pronounced circadian activity (or protein abundance). The times of peak activity or abundance were zeitgeber time (ZT) 11 (PFK), ZT 21 (PDH), and ZT 8 h (p-GS), corresponding well to transcript-based expectations (Fig. S6*C*). Because p-GS is the

inactive form of GS, it corresponds to an estimated time of peak activity around ZT 20 h for GS activity.

Hence, the time of peak activity of PFK, sometimes considered a rate-determining step in glycolysis, showed large phase lags toward two other key enzymes of glucose metabolism: GS and PDH. This finding is consistent with phase optimization for large amplitudes according to our theoretical analysis based on CRA (Fig. 5*B*): PFK and GS reactions with nearly antiphasic activities lead to maximal amplitude of the flux through both of these reactions. Furthermore, the phase difference between PFK and PDH of about 10 h implies high amplitudes for the flux through LDH at heavy exercise as well as the flux through PDH at rest. The flux through PDH at heavy workload is, however, predicted to be almost constant according to these measurements and our analysis.

Discussion

We investigated the consequences of circadian rhythms in enzyme activities for metabolite concentrations and metabolic fluxes through reactions and pathways. In particular, we investigated common pathway motifs, which are building blocks that suffice to construct almost arbitrary pathways (25). By understanding circadian control of these building blocks, one may infer the circadian control properties of much more complex pathways, such as we exemplified here with muscle glucose metabolism. A key insight was that, although metabolic reactions occur at much faster timescales than circadian rhythms, there are large time lags between enzyme activity rhythms on the one hand and concentrations and fluxes on the other hand. As a consequence, rhythmicity in fluxes and concentrations is not necessarily maximal if enzyme activities are rhythmic with the same phase, but rather, phase differences of the order of 6–12 h in enzyme activities are necessary for synergistic amplitude amplification effects. Finally, we measured enzyme activity rhythms in mouse skeletal muscle, and indeed found large phase differences in circadian enzyme activities.

The precise function of circadian rhythms for metabolism is still unclear. One concept, which we adopted in most of this study, is that a rhythmic metabolic flux is advantageous, because it provides higher energy supply at times when high demand is more likely (37). We speculate that the basal glycolytic rate is, along these lines, strongly circadian, while at the same time, retaining a constant capacity for immediate heavy workload requirement as suggested by our CRA computations and enzyme activity measurements. This view complies with the idea that the flux through a pathway is subject to evolutionary optimization, much more so than the efficiency (14). Nevertheless, another possibility is that constant fluxes and concentrations are desirable for the organism. Here, the function of rhythmic enzyme activities could be to eliminate rhythms that arise from high energy demand at times of high activity (38). In that case, for muscle glucose metabolism, environmentally dependent circadian variations in glucose supply would be superimposed on the rhythmic basal glycolysis capacity.

The theoretical insights that we derived for rhythmically modulated branching points, linear chains, and cycles are generally applicable and can be used for any reactions and pathways consisting of these building blocks. Experience from decades of work in standard MCA theory has shown that a plethora of cellular metabolic pathways can be described by the motifs studied in this work (24). However, a major bottleneck remains in the experimental identification of enzyme activities. A high-throughput method is not yet available, and measurements have to be performed for each enzyme individually, such as in this study (Fig. 5). Here, our observation that regulatory proteins rather than enzymes are the most likely points of circadian control (Fig. S1*A*) might serve as a useful guiding principle when identifying promising candidate circadian reactions based on transcriptomics or proteomics data. In future research, this approach can be combined with principles derived from CRA to extend computational methods for indirect measurement of metabolic fluxes (39) in circadian reaction networks. Moreover, the circadian regulation of other biological networks, such as signal transduction or cell-to-cell communication, is also governed by similar organization principles and can be analyzed by CRA in future research.

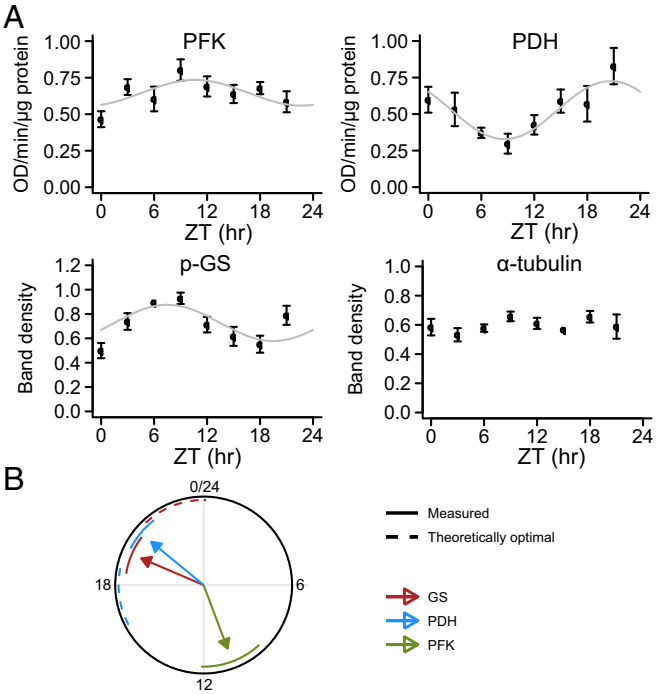

Fig. 5. Circadian activities of key enzymes in glucose metabolism. (*A*) Measurement of circadian enzyme activities in mouse muscle over a 24-h light/dark cycle. PDH and PFK enzyme activities were measured directly; p-GS (inactive fraction of total GS) and α-tubulin were analyzed by Western blot (Fig. S6). All data are based on a single experiment with six biological replicates per time point (error bars: SEM). (*B*) Illustration of measured phases (solid arrows; SEM given as circle segments) compared with theoretically optimal phases for maximal flux amplitudes through the PDH-catalyzed reaction at basal metabolism (Fig. 4*E*).

Materials and Methods

CRA. The light/dark cycle is described by a 24-h period (ZT), with lights on at ZT 0–12 h and lights off at ZT 12–24 h (Fig. 1*A*). Consider a metabolic reaction network consisting of metabolites X_k, $k = 1 \ldots M$. We describe periodically modulated reaction rate coefficients by functions of the form

$$f_i(t) = k_i[1 + A_i \cos(\omega t + \varphi_i)] \quad [1]$$

that is, by their time-averaged value (average rate coefficient) k_i and sinusoids with relative amplitude A_i, circadian frequency $\omega = 2\pi/(24\text{ h})$, and phase φ_i. By this definition, the circadian phase in hours ZT equals $-\varphi_i/\omega$. Metabolite concentrations $X_k(t)$ and fluxes $J_l(t)$ [each flux has the form $J(t) = X(t)f(t)$, representing linearized standard kinetics (12)] can be approximated by periodic modulations around the nonoscillatory steady state (21):

$$\begin{aligned} X_k(t) &= \overline{X_k}[1 + B_k \cos(\omega t + \gamma_k)] \\ J_l(t) &= \overline{J_l}[(1 + C_l \cos(\omega t + \delta_l))], \end{aligned} \quad [2]$$

where $\overline{X_k}$ and $\overline{J_l}$ are estimates for their time-averaged values. In a linear approximation, the relation between input and output amplitudes and phases can be represented by vector algebra (Fig. S1*C*). The angle of each vector represents the phase, and the length represents the relative amplitude. Each periodic reaction generates a periodic modulation in the metabolites and fluxes, with effective phases $\hat{\gamma}_i^k = \varphi_i + \hat{\varphi}_i^{X_k}$ and $\hat{\delta}_i^l = \varphi_i + \hat{\varphi}_i^{J_l}$ and

effective amplitudes $\hat{B}_i^k = A_i \hat{A}_i^{x_k}$ and $\hat{C}_i^l = A_i \hat{A}_i^{J_l}$. The combined effect of all circadian reactions giving rise to the final values B_k, C_l, γ_k, δ_l is given by superposition in phase space. Importantly, because the circadian frequency is typically much smaller than most metabolic reaction rate coefficients (Fig. S1*B*), we applied the assumption

$$\omega \ll k_i, \qquad [3]$$

which allowed us to derive simple expressions for the response coefficients of metabolic motifs (*SI Appendix*). For detailed derivations and Mathematica notebooks implementing CRA, see *SI Text* and Datasets S1 and S2.

Optimal Phase Difference and Effect Size. The amplitudes B_k and C_l (Eq. **2**) of the metabolites and fluxes in periodically modulated metabolic networks attain maximal values when $\hat{\gamma}_1^k = \hat{\gamma}_2^k = \ldots = \hat{\gamma}_M^k$ and $\hat{\delta}_1^l = \hat{\delta}_2^l = \ldots = \hat{\delta}_N^l$, respectively. We studied metabolic motifs with two circadian reactions (Fig. 2 and Fig. S2) with phase difference $\Delta\varphi = \varphi_2 - \varphi_1$. The optimal phase difference for maximal metabolite or flux amplitude is $\Delta\varphi_{\text{opt}}^{x_k} = \hat{\varphi}_1^{x_k} - \hat{\varphi}_2^{x_k}$, $\Delta\varphi_{\text{opt}}^{J_l} = \hat{\varphi}_1^{J_l} - \hat{\varphi}_2^{J_l}$. If this optimal phase difference is achieved, then the corresponding (maximal) amplitude is given by $B_k^{\max} = A_1 \hat{A}_1^{x_k} + A_2 \hat{A}_2^{x_k}$, and the minimal amplitude is reached when the two effective phases are misaligned, which yields $B_k^{\min} = \sqrt{(A_1 \hat{A}_1^{x_k})^2 - (A_2 \hat{A}_2^{x_k})^2}$ (analogously for the fluxes). We defined the effect size (Fig. 2*C* and Fig. S2*C*) as $S_{\text{effect}}^{x_k} = B_k^{\max} - B_k^{\min}$, $S_{\text{effect}}^{J_l} = C_l^{\max} - C_l^{\min}$.

In many cases, several enzymes with moderate individual activity rhythms may together cause larger rhythms in metabolite concentrations and fluxes, provided that the enzyme activity phases are properly aligned (*SI Text*).

Experimental Procedures, Data Analysis, and Mathematical Models. C57BL/6J mice (male; 8 wk old) were entrained for 2 wk to 12-h/12-h light/dark cycles before being euthanized at time points ZT 0, 3, 6, . . ., 24 h ($n = 6$). All animal studies were conducted in accordance with our regional committee for ethics in animal experimentation. The activities of PDH and PFK were assayed using the PDH Activity Assay Kit from EMD Millipore (Merck KGaA) and the PFK Colorimetric Assay Kit from BioVision according to the manufacturers' instructions. The activity of GS was monitored by Western blot against anti–p-GS antibody.

To identify circadian transcript abundances, we used published microarray data (6, 18, 32) and selected carbohydrate enzyme regulatory proteins and carbohydrate metabolic enzymes by corresponding GO terms. Linearized rate coefficients for enzyme-catalyzed reactions (Fig. S1*B*) were obtained from a collection of enzyme k_{cat} and K_{m} values (40). Phases (with SEM) and amplitudes for all data were estimated using harmonic regression (3).

Mathematical models of metabolic network motifs as well as the reduced models of the TCA cycle and glycolysis were obtained by mass action kinetics (equations in *SI Materials and Methods* or *SI Appendix*), with average reaction rate coefficients set to 10 h^{-1} (compare Fig. S1*B*) and relative amplitudes of 0.5 unless stated otherwise. For variations in K_{eq}, k^+ was held constant at 300 h^{-1}, and k^- was varied.

Extended methods are available in *SI Materials and Methods*.

ACKNOWLEDGMENTS. We thank Sarah Lück and Paul Thaben for help with mouse experiments, Hanspeter Herzel and Wolfram Liebermeister for discussions, and Satwik Rajaram and Marion Langen for critical reading of the manuscript. This work was supported by Research Fellowship of the Deutsche Forschungsgemeinschaft Grant TH 1861/1-1 (to K.T.) and German Ministry for Education and Research Grant 0315899 (to P.O.W.).

1. Green CB, Takahashi JS, Bass J (2008) The meter of metabolism. *Cell* 134:728–742.
2. Lück S, Westermark PO (2015) Circadian mRNA expression: Insights from modeling and transcriptomics. *Cell Mol Life Sci* 73:497–521.
3. Lück S, Thurley K, Thaben PF, Westermark PO (2014) Rhythmic degradation explains and unifies circadian transcriptome and proteome data. *Cell Rep* 9:741–751.
4. Mauvoisin D, et al. (2014) Circadian clock-dependent and -independent rhythmic proteomes implement distinct diurnal functions in mouse liver. *Proc Natl Acad Sci USA* 111:167–172.
5. Robles MS, Cox J, Mann M (2014) In-vivo quantitative proteomics reveals a key contribution of post-transcriptional mechanisms to the circadian regulation of liver metabolism. *PLoS Genet* 10:e1004047.
6. Zhang R, Lahens NF, Ballance HI, Hughes ME, Hogenesch JB (2014) A circadian gene expression atlas in mammals: Implications for biology and medicine. *Proc Natl Acad Sci USA* 111:16219–16224.
7. Feuers RJ, et al. (1986) The effects of various lighting schedules upon the circadian rhythms of 23 liver or brain enzymes of C57BL/6J mice. *Chronobiol Int* 3:221–235.
8. Civen M, Ulrich R, Trimmer BM, Brown CB(1967) Circadian rhythms of liver enzymes and their relationship to enzyme induction. *Science* 157:1563–1564.
9. Dallmann R, Viola AU, Tarokh L, Cajochen C, Brown SA (2012) The human circadian metabolome. *Proc Natl Acad Sci USA* 109:2625–2629.
10. Fustin JM, et al. (2012) Rhythmic nucleotide synthesis in the liver: Temporal segregation of metabolites. *Cell Rep* 1:341–349.
11. Adamovich Y, et al. (2014) Resource: Circadian clocks and feeding time regulate the oscillations and levels of hepatic triglycerides. *Cell Metab* 19:319–330.
12. Cornish-Bowden A (2012) Fundamentals of Enzyme Kinetics (Wiley-Blackwell, Weinheim, Germany), 4th Ed.
13. Zaslaver A, et al. (2004) Just-in-time transcription program in metabolic pathways. *Nat Genet* 36:486–491.
14. Waddell TG, Repovic P, Melendez-Hevia E, Heinrich R, Montero F (1997) Optimization of glycolysis: A new look at the efficiency of energy coupling. *Biochem Edu* 25:204–205.
15. Schwanhausser B, et al. (2011) Global quantification of mammalian gene expression control. *Nature* 473:337–342.
16. Oster H, et al. (2006) The circadian rhythm of glucocorticoids is regulated by a gating mechanism residing in the adrenal cortical clock. *Cell Metab* 4:163–173.
17. Panda S, et al. (2002) Coordinated transcription of key pathways in the mouse by the circadian clock. *Cell* 109:307–320.
18. Dyar KA, et al. (2014) Muscle insulin sensitivity and glucose metabolism are controlled by the intrinsic muscle clock. *Mol Metab* 3:29–41.
19. Eckel-Mahan KL, et al. (2012) Coordination of the transcriptome and metabolome by the circadian clock. *Proc Natl Acad Sci USA* 109:5541–5546.
20. Clarke CF, Fogelman AM, Edwards PA (1984) Diurnal rhythm of rat liver mRNAs encoding 3-hydroxy-3-methyl-glutaryl coenzyme A reductase. *J Biol Chem* 259:10439–10447.
21. Ingalls BP (2004) A frequency domain approach to sensitivity analysis of biochemical networks. *J Phys Chem B* 108:1143–1152.
22. Kacser H, Burns JA (1973) The control of flux. *Symp Soc Exp Biol* 27:65–104.
23. Heinrich R, Rapoport TA (1974) A linear steady-state treatment of enzymatic chains. General properties, control and effector strength. *Eur J Biochem* 42:89–95.
24. Heinrich R, Rapoport SM, Rapoport TA (1977) Metabolic regulation and mathematical models. *Prog Biophys Mol Biol* 32:1–82.
25. Rohwer JM, Schuster S, Westerhoff HV (1996) How to recognize monofunctional units in a metabolic system. *J Theor Biol* 179:213–228.
26. Heinrich R, Holzhutter HG, Schuster S (1987) A theoretical approach to the evolution and structural design of enzymatic networks; linear enzymatic chains, branched pathways and glycolysis of erythrocytes. *Bull Math Biol* 49:539–595.
27. Owen OE, Kalhan SC, Hanson RW (2002) The key role of anaplerosis and cataplerosis for citric acid cycle function. *J Biol Chem* 277:30409–30412.
28. Neufeld-Cohen A, et al. (2016) Circadian control of oscillations in mitochondrial rate-limiting enzymes and nutrient utilization by PERIOD proteins. *Proc Natl Acad Sci USA* 113(12):E1673–E1682.
29. Nelson DL, Cox MM (2013) *Lehninger: Principles of Biochemistry* (W. H. Freeman, New York), 6th Ed.
30. Jucker BM, Rennings AJ, Cline GW, Petersen KF, Shulman GI (1997) In vivo NMR investigation of intramuscular glucose metabolism in conscious rats. *Am J Physiol* 39–48.
31. Bonen A, McDermott JC, Tan MH (1990) Glycogenesis and glyconeogenesis in skeletal muscle: Effects of pH and hormones. *Am J Physiol* 258:693–700.
32. Miller BH, et al. (2007) Circadian and CLOCK-controlled regulation of the mouse transcriptome and cell proliferation. *Proc Natl Acad Sci USA* 104:3342–3347.
33. Klipp E, Heinrich R, Holzhütter HG (2002) Prediction of temporal gene expression. Metabolic opimization by re-distribution of enzyme activities. *Eur J Biochem* 269:5406–5413.
34. Spriet LL, Howlett RA, Heigenhauser GJ (2000) An enzymatic approach to lactate production in human skeletal muscle during exercise. *Med Sci Sport Exerc* 32:756–763.
35. Thaben PF, Westermark PO (2014) Detecting rhythms in time series with RAIN. *J Biol Rhythms* 29:391–400.
36. Wu G, Anafi RC, Hughes ME, Kornacker K, Hogenesch JB (2016) MetaCycle: An integrated R package to evaluate periodicity in large scale data. *Bioinformatics* 32:3351–3353.
37. Van der Vinne V, et al. (2014) Cold and hunger induce diurnality in a nocturnal mammal: Function and mechanism. *Proc Natl Acad Sci USA* 111:15256–15260.
38. Lamia KA, Storch KF, Weitz CJ (2008) Physiological significance of a peripheral tissue circadian clock. *Proc Natl Acad Sci USA* 105:15172–15177.
39. Cascante M, Marin S (2008) Metabolomics and fluxomics approaches. *Essays Biochem* 45:67–82.
40. Bar-Even A, et al. (2011) The moderately efficient enzyme : Evolutionary and physicochemical trends shaping enzyme parameters. *Biochemistry* 50:4402–4410.
41. Easterby JS (1981) A generalized theory of the transition time for sequential enzyme reactions. *Biochem J* 199:155–161.